The Use of a Filter Bank and the Wigner–Ville Distribution for Time–Frequency Representation

Farook Sattar and Göran Salomonsson

***Abstract*—We present a new method for time–frequency representation, which combines a filter bank and the Wigner–Ville distribution (WVD). The filter bank decomposes a multicomponent signal into a number of single component signals before the WVD is applied. Cross-terms as well as noise are reduced significantly, whereas high time–frequency concentration is attained. Properties of the proposed time–frequency distribution (TFD) are investigated, and the requirements for the filter bank to fulfil these are given. The ability of the proposed *non-Cohen's class* TFD to reduce cross-terms as well as noise as well as its ability to approximately reconstruct signals are illustrated by examples. The results are compared with those from WVD, the Choi–Williams distribution (CWD), and spectrogram.**

***Index Terms*— Signal reconstruction, time–frequency analysis, time–frequency distribution, time–frequency signal representations.**

I. Introduction

Many common signals have time-varying spectra. A speech signal is one example belonging to this class. Although the Fourier transform (FT) of such a signal contains all information about its behavior in the time domain, it does not tell us about the time-local properties of the signal. Thus, there is a need for a joint time–frequency distribution (TFD).

The short-time Fourier transform (STFT) is one of the earliest methods used for time–frequency analysis (TFA). A moving window cuts out a slice of the signal, and the FT of this slice gives the local properties of the signal. The STFT can be interpreted as the output signals from a bandpass filter bank. The spectrogram, which is the magnitude squared of the STFT, is used for the analysis of nonstationary signals, e.g., speech signals. The result depends strongly on the choice of the window function, and as a rule, the concentration is poor [1], [2].

Another commonly used TFD is the Wigner–Ville distribution (WVD) [1], [2]. The WVD exhibits the highest signal energy concentration in the time–frequency plane for linearly modulated signals, but major problems are artifacts in the case of nonlinearly frequency modulated signals and the presence of cross-terms for multicomponent signals. WVD is noisy due to the cross-terms, and furthermore, noise can appear in the time–frequency plane at times when there is no noise in the signal.

The objective of this correspondence is to investigate a new TFD *of non-Cohen's class* that avoids the drawbacks inherent in the WVD and at the same time retains the advantages of the spectrogram and the WVD. Above all, the TFD has to reduce cross-terms and have a high energy concentration of the signal. This is done by combining a bandpass filter bank and the WVD. The purpose of the filter bank is to decompose a multicomponent signal into a number of single component signals. Cross-terms and the noisy character of the following WVD's will then be diminished. The filter bank gives a controlled frequency resolution, whereas the WVD retains the energy concentration in the time–frequency plane. An analysis of the proposed TFD is done, and a demand on the filter bank is found in order to obtain the desired properties of frequency and time marginals. A method for an approximate signal reconstruction is suggested. The TFD is illustrated by some examples that are well known from the literature. It is also compared with the WVD, the Choi–Williams distribution (CWD) [2], [5], the spectrogram [2], [6] and a smoothed pseudo-WVD, which are all belong to *Cohen's Class*.

Manuscript received May 23, 1996; revised October 30, 1998. The associate editor coordinating the review of this paper and approving it for publication was Dr. Nurgun Erdol.

F. Sattar was with the Department of Applied Electronics, Signal Processing Group, Lund University, Lund, Sweden. He is now with with the School of Electrical and Electronic Engineering, Nanyang Technological University, Singapore.

G. Salomonsson is with the Department of Applied Electronics, Signal Processing Group, Lund University, Lund, Sweden.

Publisher Item Identifier S 1053-587X(99)03686-7.

II. The Combination of Filter Bank and WVD

In order to avoid the drawbacks inherent in the WVD, a combination of a bandpass filter bank and the WVD is investigated. The aim of the filter bank is to decompose a multicomponent signal into a number of single component signals. Cross-terms and the noisy character of the following WVD's will then be diminished. An analysis of the combination will follow.

A. The Bandpass Filter Bank

The impulse responses of the subfilters of a uniform bandpass filter bank are given by

$$h_i(t) = h(t)e^{j2\pi f_i t}, \qquad i = 1, \cdots, M. \tag{1}$$

In (1), $h(t)$ is the real-valued impulse response of a prototype lowpass filter, and M is the number of subfilters. Each subfilter is obtained by modulating the lowpass filter by a complex exponential with the normalized frequency $f_i = i/L, i = 1, \cdots, M$. The transfer functions of the subfilters are

$$H_i(f) = H(f - f_i), \qquad i = 1, \cdots, M. \tag{2}$$

The separation in the frequency domain of the subfilters is determined by L. The input real signal $s(t)$ to the filter bank is bandlimited to the normalized frequency interval $[1/L, 1/2 - 1/L]$. Thus, the spectrum of $s(t)$ is covered by the subfilters indexed $i = 1, \cdots, L/2 - 1$.

The output from the ith subfilter is

$$z_i(t) = s(t) * h_i(t) \tag{3}$$

where "$*$" denotes the convolution operator. The complex signal $z_i(t)$ becomes analytic, provided the Fourier transform of $z_i(t), Z_i(f) = 0$ for $f < 0$. This will occur for all subfilters if $H(f) = 0, |f| > 1/L$. The choice of the prototype impulse response $h(t)$ is constrained by conditions on the output of the filter bank or on the TFD, which is obtained by the combination of the filter bank and the WVD. Two conditions have been investigated. In the first case, $h(t)$ is constrained to give perfect reconstruction i.e, $\Re\{\sum_{i=1}^{L/2} z_i(t)\} = s(t)$, where $\Re\{\cdot\}$ means "real part of." The perfect reconstruction can then be achieved by a filter with impulse response $h(t)$ that satisfies [7]

$$\begin{aligned} h(0) &= 1/L \\ h(lL) &= 0 \quad \forall l \neq 0 \end{aligned} \tag{4}$$

which, in the frequency domain, corresponds to

$$\left| \sum_{i=0}^{M} H(f - f_i) \right| = 1, \qquad 0 \leq f \leq M/L. \tag{5}$$

In the second case, $h(t)$ is constrained by the demand that the TFD satisfies the time and frequency marginals. Then, $H(f)$ has to fulfil

$$\sum_{i=0}^{M} |H(f-f_i)|^2 = 1, \qquad 0 \le f \le M/L. \tag{6}$$

The filters that satisty (6) are said to be power complementary (PC) filters in [11]. In order to have the PC property for perfect reconstruction, the filter bank structure/design are also discussed in [11]–[13].

The complex filter bank can be implemented by using two filter banks with impulse responses of the subfilters given by

$$\begin{aligned} h_i^c(t) &= h(t)\ \cos 2\pi f_i t \\ h_i^s(t) &= h(t)\ \sin 2\pi f_i t \qquad i = 1, \cdots, M. \end{aligned} \tag{7}$$

The complex combination of their outputs gives the analytic output signal $z_i(t)$ if $|H(f)| = 0, f > 1/L$ [5].

The frequency resolution in the time–frequency plane can easily be changed by adding neighboring subfilters of the uniform filter bank. For example, an octave filter bank can be designed from the uniform bank by adding the impulse responses from $2^j, j = 0, 1, \cdots, N$ neighboring subfilters, and the outputs from the new subfilters are still analytic signals as long as the condition $H(f) = 0, |f| > 1/L$ is valid. The proposed filter bank is thus flexible for tiling the time–frequency plane by scaling due to (5). Thus, the filter bank can be matched to a larger number of applications, e.g., from tracking periodic signals with varying frequency to the analysis of transient signals. Tiling of the time–frequency plane may also be done by using metaplectic transforms [14].

B. WVD of a Subband Signal

The generalized WVD (GWVD) is defined by

$$W_q(t,f) = \int z^q\left(t+\frac{\tau}{2q}\right) z^{*q}\left(t-\frac{\tau}{2q}\right) e^{-j2\pi f\tau}\, d\tau \tag{8}$$

where

- $z(t)$ complex-valued signal;
- $z^*(t)$ complex conjugate of $z(f)$;
- q positive integer [4] (the range of all integrations is from $-\infty$ to ∞ unless otherwise stated).

The ordinary WVD is obtained for $q = 1$ [2]. Moreover, the WVD of a linear filtering operation is the convolution of the WVD of the signal and of the filter in the time domain. If the convolution of $s(t)$ and $h(t)$ is $y(t) = \int s(\tau)h(t-\tau)\, d\tau$, then the WVD of $y(t)$ is

$$W_y(t,f) = \int W_s(u,f) W_h(t-u,f)\, du. \tag{9}$$

By using the definition in (8) with $q = 1$ and (9), the WVD for the signal of the ith channel $z_i(t)$ is given by

$$\begin{aligned} W_i(t,f) &= \iint s(u+\xi/2)s^*(u-\xi/2) \\ &\quad \cdot G_i(t-u, f-f_i) e^{-j2\pi f\xi}\, du\, d\xi \\ &= \int W_s(u,f) G_i(t-u, f-f_i)\, du \\ &\qquad i = 1, \cdots, M \end{aligned} \tag{10}$$

where

$$G_i(t, f-f_i) = \int h(t+\eta/2)h(t-\eta/2) e^{-j2\pi(f-f_i)\eta}\, d\eta. \tag{11}$$

In (10), the smoothing of $W_s(t,f)$ by the kernel $G_i(t, f-f_i)$ is done only in the time domain. The smoothing in frequency depends on the bandwidth $1/L$ of the prototype filter. Other representations of the kernel $G_i(t, f-f_i)$ can be obtained as Fourier transform (FT) with respect to either the time variable t or the frequency variable f. By taking the inverse Fourier transform (IFT) of $G_i(t, f-f_i)$ with respect to time t and frequency f, we can find the kernel in the ambiguity plane (θ, τ) as

$$\begin{aligned} g_i(\theta,\tau) &= e^{j2\pi f_i\tau} \int h(t+\tau/2)h(t-\tau/2) e^{-j2\pi\theta t}\, dt \\ &= g_h(\theta,\tau) e^{j2\pi f_i\tau} \end{aligned} \tag{12}$$

where $g_h(\theta,\tau)$ is the ambiguity function for the impulse response $h(t)$ of the prototype filter.

The time-lag function $\psi_i(t,\tau)$ and spectral correlation function $\Psi_i(\theta,f)$ can also be obtained from $G_i(t, f-f_i)$ by the IFT with respect to f and the FT with respect to t [8]. In (12), it is noticed that the controlling parameter of the kernel $g_h(\theta,\tau)$ is the shape and bandwidth of the lowpass filter $h(t)$.

C. The TFD and its Kernels

The TFD of the input signal $s(t)$ is defined as a linear combination of the individual TFD $W_i(t,f)$ and is given by

$$T(t,f) = \sum_{i=1}^{M} \gamma_i W_i(t,f) \tag{13}$$

where the γ_i's represent scalar weights. By choosing different γ_i's, the entire time–frequency plane can be segmented, or specific frequency regions of interest can be selected. In our analysis, the values of all γ_i's are equal to 1. Then, by using (10), the TFD $T(t,f)$ can be rewritten as

$$T(t,f) = \int W_s\ (u,f) G(t-u, f-\overline{f})\, du \tag{14}$$

where

$$\begin{aligned} G(t, f-\overline{f}) &= \sum_{i=1}^{M} G_i(t, f-f_i) \\ &= \int h(t+\eta/2)h(t-\eta/2) \\ &\quad \cdot \frac{\sin \pi M\eta/L}{\sin \pi\eta/L} e^{-j2\pi(f-\overline{f})\eta}\, d\eta. \end{aligned} \tag{15}$$

In (15), $\overline{f} = (M+1)/2L$, and $G(t,f)$ is real valued, which results in the TFD $T(t,f)$ in (14) being real (see Appendix A). Thus, the WVD of the signal $s(t)$ is smoothed in the time domain by the signal-independent kernel $G(t, f-\overline{f})$ with the property of $G(t, f-\overline{f}) = 0$, $f < 0$. The ambiguity function corresponding to $G(t, f-\overline{f})$ is

$$\begin{aligned} g(\theta,\tau) &= \sum_{i=1}^{M} g_i(\theta,\tau) \\ &= g_h(\theta,\tau)\ \frac{\sin \pi M\tau/L}{\sin \pi\tau/L} e^{j\pi(M+1)\tau/L}. \end{aligned} \tag{16}$$

The time-lag function is

$$\psi(t,\tau) = \psi_h(t,\tau)\ \frac{\sin \pi M\tau/L}{\sin \pi\tau/L} e^{j\pi(M+1)\tau/L}. \tag{17}$$

Finally, the spectral correlation function $\Psi(\theta,f)$ in the (θ,f) domain can be obtained as the Fourier transform of $g(\theta,\tau)$ in (16) with respect to τ.

D. Properties of the TFD

The TFD needs to fulfil a number of desirable properties [8]. It has already been mentioned that the TFD in (14) is real valued (see Appendix A). The TFD in (13) will also satisfy the frequency marginal

$$\int T(t,f)\,dt = |S(f)|^2 \tag{18}$$

if $H(f)$ fulfils the condition shown in (6) (see Appendix A).

In order to obtain the time marginal, the TFD is integrated over frequency, and a function $P(t)$ is found as

$$P(t) = \int T(t,f)\,df = \sum_{i=0}^{2M} |z_i(t)|^2 = \sum_{i=0}^{2M} |h_i * s|^2. \tag{19}$$

Equation (19) will approximately fulfil the time marginal, that is,

$$P(t) \approx |s(t)|^2 \tag{20}$$

when L is less than, e.g., $L \leq 32$ (see Appendix A). This agrees with the behavior of the kernels since L becomes large, e.g., $L = 64$, the kernel bandwidth is narrower, and the TFD $T(t,f)$ then behaves more like a spectrogram, which do not satisfy the time marginal [8].

The approximation in (20) will be exemplified by an input chirp signal $s(t)$ in a time interval $(0,T)$ and the prototype filter function $|H(f)| = \cos((\pi/2)|f|L)$, $|f| < 1/L$. A normalized approximation error ε, which is defined as

$$\varepsilon = \frac{\int_0^T |P(t) - |s(t)|^2|\,dt}{\int_0^T s^2(t)\,dt} \tag{21}$$

is calculated (see Table I). The error ε is given in Table I for different values of L. It is seen that the approximation in (20) deteriorates as L increases. When the frequency marginal, as above, is satisfied, the total energy E, which is expressed in terms of the distribution, can be given by

$$E = \iint T(t,f)\,dt\,df = \int |S(f)|^2\,df = \int s^2(t)\,dt. \tag{22}$$

The TFD $T(t,f)$ satisfies the property of time shift [6]

$$\tilde{s}(t) = s(t-t_0) \Rightarrow T_{\tilde{s}}(t,f) = T_s(t-t_0,f) \tag{23}$$

since the filter bank decomposition does not depend on time t, and the WVD is a shift-invariant TFD. A similar relationship for the frequency shift does not hold since the filter bank "quantizes" the frequency plane into overlapping regions of width $2/L$. Modulation of the signal $e^{j2\pi f_o t}$ thus results in a frequency shift of the entire $T(t,f)$ plane only when the frequency shift f_0 corresponds to the discrete center frequency of the filter. That is

$$\tilde{s}(t) = s(t)e^{j2\pi f_0 t} \Rightarrow \begin{cases} T_{\tilde{s}}(t,f) = T_s(t,f-f_0), & \text{if } f_0 = f_i = i/L \\ & i = 1,\cdots,M \\ \neq T_s(t,f-f_0), & \text{otherwise.} \end{cases} \tag{24}$$

The presented TFR thus does not belong to the Cohen's class since it is not frequency shift invariant.

E. A Comparison with a Smoothed Pseudo-WVD

The $T(t,f)$ will be compared with a TFR $Q(t,f)$ of Cohen's class, which has a kernel $g(\theta,\tau)$ given by

$$g(\theta,\tau) = \boldsymbol{H}(\theta). \tag{25}$$

TABLE I
NORMALIZED APPROXIMATION ERROR ε FOR DIFFERENT VALUES OF L

L	Error, ε
4	0.0049
8	0.0106
16	0.0270
32	0.0754
64	0.2425

The $Q(t,f)$ is defined as

$$Q(t,f) = \int \boldsymbol{H}(\theta)\,\text{STFT}(t,f+\theta/2) \cdot \text{STFT}^*(t,f-\theta/2)e^{j2\pi\theta t}\,d\theta \tag{26}$$

where STFT is the short-time Fourier transform [6]. The resulting distribution is a frequency-domain analog to the smoothed pseudo WVD (SPWD). It first performs the time direction smoothing via STFT followed by frequency direction smoothing with $\boldsymbol{H}(\theta)$. The sequence of smoothing is just opposite for $T(t,f)$, where the frequency direction smoothing is done by convolving the input signal with a bandpass filter bank.

The $Q(t,f)$ is frequency-shift invariant. It lies in between the spectrogram and pseudo Wigner–Ville distribution like the $T(t,f)$. It is possible to trade off between energy concentration and cross-term reduction by the choice of the bandwidth of $H(\theta)$. This method can reduce cross-terms efficiently as it is done by the $T(t,f)$. However, neither the time marginal nor the frequency marginal property can be preserved (frequency marginal property can be fulfiled if an infinite-length Fourier transform is used in place of the STFT). Moreover, the method has also limitations in tiling the time–frequency plane due to the fixed bandwidth of the kernel $H(\theta)$.

F. An Approximate Method for Signal Reconstruction

The proposed TFD in (14) is a convolution in the time domain between the WVD $W_s(t,f)$ of the signal $s(t)$ and the kernel $G(t,f-\overline{f})$, which is given by (15). For large values of M, the kernel can be rewritten as [cf. (A.10)]

$$\begin{aligned} G(t,f-\overline{f}) &\approx L\int h(t+\eta/2)h(t-\eta/2) \cdot \sum_l \delta(\eta+lL)e^{-j2\pi(f-\overline{f})\eta}\,d\eta \\ &= L\{h^2(t) + 2h(t+L/2)h(t-L/2) \cdot \cos(2\pi fL)\} \sqcap (f-\overline{f}) + \epsilon(t,f-\overline{f}) \end{aligned} \tag{27}$$

where

$$\sqcap(f) = \begin{cases} 1, & |f| < M/L = \overline{f} \\ 0, & \text{elsewhere} \end{cases} \tag{28}$$

and $\epsilon(t,f-\overline{f})$ is the remainder term having small value compared with the other terms in $G(t,f-\overline{f})$. The kernel is approximated by the first two terms in (27). The approximation is bandlimited to $\theta \in (-2/L, 2/L)$ since the bandwidth of $h(t)$ is $1/L$, and it is also periodic in f with the period $1/L$.

An approximate inverse filter $b(t,f)$ to $G(t,f-\overline{f})$ is calculated for each f. This can be done either in the frequency domain, the θ-domain, finding a Wiener solution, or in the time domain by using a squared error criterion. In the later case, the impulse response $b(t,f)$ of the inverse filter will fulfil the condition

$$G(t,f-\overline{f}) * b(t,f) = p(t) \tag{29}$$

where $*$ denotes convolution in the time domain for a given value of f. The pulse $p(t)$ is independent of f, and its bandwidth is less than or equal to $2/L$. For example, we have chosen it to be

$$p(t) = \frac{\sin(2\pi t\beta/L)}{\pi t}\,\frac{\cos(\alpha\pi t\beta/L)}{1-(2\alpha t\beta/L)^2}. \tag{30}$$

The amplitude function that corresponds to (30) is constant in the frequency interval $(0, \beta/L)$ and then decreases and becomes zero at frequency $\theta = (\alpha+\beta)/2$. The solution of (29) can be found in discrete time, in which (29) is rewritten as

$$\tilde{G}_f b_f = p \tag{31}$$

where

$$\tilde{\boldsymbol{G}}_{\boldsymbol{f}} = \begin{bmatrix} G_f(1) & 0 & \cdots & 0 \\ G_f(2) & G_f(1) & \ddots & 0 \\ \vdots & \vdots & \ddots & \vdots \\ G_f(P) & G_f(P-1) & \vdots & G_f(1) \\ \vdots & \vdots & \cdots & \vdots \\ G_f(N) & G_f(N-1) & \cdots & G_f(N-P+1) \\ 0 & G_f(N) & \cdots & G_f(N-P+2) \\ \vdots & \vdots & \ddots & \vdots \\ 0 & 0 & \cdots & G_f(N) \end{bmatrix}$$

$$\boldsymbol{b}_f = \begin{bmatrix} b_f(1) \\ b_f(2) \\ \vdots \\ b_f(P) \end{bmatrix}; \quad \boldsymbol{p} = \begin{bmatrix} p(1) \\ p(2) \\ \vdots \\ p(N+P-1) \end{bmatrix}. \tag{32}$$

The matrix $\tilde{G}_f$ at each frequency f has a size of $(N+P-1)\times(P)$, b_f is a $(P)\times(1)$ vector, and p is a vector of size $(N+P-1)\times(1)$. After sampling, all signals have been truncated by a Tukey window. By using the pseudoinverse $\tilde{G}_f^{\#} = V\,\Sigma^{-1}U^T$ of $\tilde{G}_f = U\Sigma V^T$, the impulse response of the inverse filter is obtained as [9]

$$\boldsymbol{b}_f = \tilde{\boldsymbol{G}}_f^{\#}\boldsymbol{p} = \sum_{i=1}^{r}\frac{(u_i^T p)}{\sigma_i}v_i \tag{33}$$

where $r \le \text{rank}\{\tilde{G}_f\}$, u_i's and v_i's are the ith orthonormal eigenvectors, which are associated with the nonzero eigenvalues of σ_i, and v_i^T is the transpose of v_i. The estimated inverse filter $b(t,f)$ is inserted in (14), giving

$$T(t,f) * b(t,f) = W_s(t,f) * G(t, f-\overline{f}) * b(t,f). \tag{34}$$

Due to the design of $b(t,f)$, the WVD of $s(t)$ will still be bandlimited by a filter with a bandwidth less than or equal to $2/L$. Thus, the WVD of $s(t)$ will only approximately correspond to the left-hand side of (34), and the approximation deteriorates with increasing L. This agrees with the discussion of the properties of the kernels, where it was found that the $T(t,f)$ gradually passes from the WVD to the spectrogram for increasing L. Thus, the reconstructed signal $\hat{s}(t)$ can only approximately be obtained from [1], [10]

$$\begin{aligned}\hat{s}(t) &= \frac{1}{\hat{s}^*(0)}\int W_s(t/2,f)e^{j2\pi ft}\,df \\ &= \frac{1}{\hat{s}^*(0)}\int W(t/2,f) * b(t/2,f)e^{j2\pi ft}\,df \\ &= \frac{1}{\hat{s}^*(0)}\iint W(2\theta,f)B(2\theta,f)e^{j2\pi\theta t}e^{j2\pi ft}\,d\theta\,df. \end{aligned}\tag{35}$$

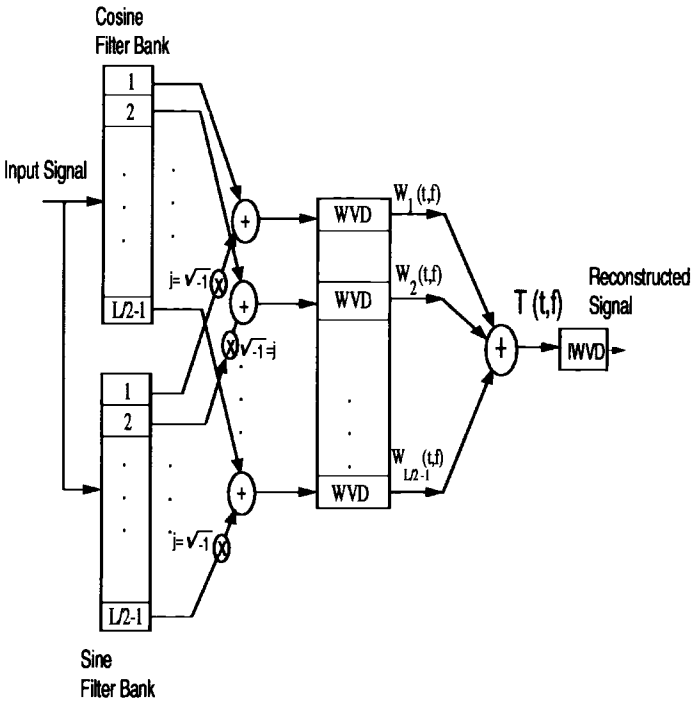

Fig. 1. Block diagram for the proposed time–frequency distribution method.

G. The Discrete Version

The discrete-time formulations, corresponding to the TFD $T(t,f)$, are given in the following, where the sampling frequency must be at least twice the maximum frequency to satisfy the Nyquist criterion. The signal $s(n)$ has to be bandlimited in the frequency interval $[1/L, 1/2-1/L]$. In discrete time, the WVD can be defined as [1]

$$\begin{aligned}W_i(n,k) = &\sum_{m=-(K-1)/2}^{(K-1)/2} w(m)z_i(n+m) \\ &\cdot z_i^*(n-m)e^{-j4\pi mk/K}\end{aligned}\tag{36}$$

where $z_i(n)$ is the analytic signal at the ith frequency band and n, $k(0 \le k \le K)$ and m are the discrete variables corresponding to time, frequency, and lag of (8), whereas $w(m)$ is a real window [1].

The final TFD is

$$T(n,k) = \sum_{i=1}^{M}\gamma_i W_i(n,k). \tag{37}$$

In discrete form, the TFD in (26) can also be written as

$$\begin{aligned}Q(n,k) = &\sum_{p=-l/2}^{l/2}\boldsymbol{H}(p)\ \text{STFT}(n,k+p) \\ &\cdot \text{STFT}^*(n,k-p)e^{j4\pi pn/l}\end{aligned}\tag{38}$$

where

$$\text{STFT}(n,k) = \sum_{m=-K/2}^{K/2} w(m)s(n+m)e^{-j2\pi mk/K.} \tag{39}$$

III. Numerical Examples

The following examples illustrate the use of the TFD method for which the block diagram is shown in Fig. 1, and the results are compared with the spectrogram and the CWD. For the proposed TFD, the filter bank plays an important role since the number of subfilters L and the prototype impulse response $h(t)$ decide the character of

the kernels. Two prototype filters, which have the frequency function $H(f)$ and fulfil the condition shown in (6), are provided. The first one is given by

$$|H(f)|^2 = 1 - L|f| \qquad |f| \le 1/L \tag{40}$$

and the second one belongs to the class of raised cosine functions given as

$$|H(f)|^2 = \cos^2 \frac{\pi}{2}\,|f|L \qquad |f| \le 1/L \tag{41}$$

where the number L of the subfilters is a parameter that controls the bandwidth of the filters as well as the character of the kernel.

In the following examples, the two filter banks that are generated from the prototype filter with $H(f)$ in (40) and in (41) are denoted by FB1 (Filter Bank 1) and FB2 (Filter Bank 2), respectively. For convenience, the proposed TFD corresponding to FB1 and FB2 are represented by $T1$ and $T2$, respectively. In addition, for the spectrogram, the impulse response of the filter with $|H(f)|^2$ is used as the window function. For the WVD calculation, a rectangular window $w(n)$ is used throughout.

Example 1—Cross-term and Noise Reduction: In this example, first, we consider cross-term reduction for a multicomponent signal. The signal is the sum of two linearly modulated signals given by

$$s(n) = 4\cos\left(\frac{2\pi}{N}\,(n/8)n\right) + 4\cos\left(\frac{2\pi}{N}\,((2N-n)/8)n\right) \qquad n = 0, \cdots, N-1. \tag{42}$$

The parameters used in this example are $K = 128$ and $N = 512$. The value of the controlling parameters for the proposed distribution and the CWD are chosen as $L = 32$ and $\sigma = 0.5$ [3], respectively. For the TFD Q, a rectangular window $\boldsymbol{H}(\theta)$ with width $l = 7$ is used, and a Hamming window is used for the corresponding STFT calculation. For the spectrograms, which are shown in Fig. 2(c) and (d), the impulse responses of the transfer functions $|H(f)|^2$, which are given in (40) and (41), are chosen for the window functions. The results of the WVD, CWD, spectrograms, and proposed TFD are presented in Fig. 2 [contour plots are shown in Fig. 2(a)–(g)]. Compared with the CWD and the spectrogram, the proposed TFD reduces the cross-terms but retains the high energy concentration of the signal. On the other hand, the $T(t, f)$ can perform comparably with the TFD Q.

Second, we have shown the noise reduction by using a linearly frequency modulated signal corrupted by additive white Gaussian noise v with SNR = 3 and 0 dB. The SNR (in decibels) is defined as 10 $\log_{10}(\sigma_s^2/\sigma_v^2)$, where σ_s^2 and σ_v^2 are the variances of $s(n)$ and $v(n)$, respectively. The example is illustrated by using the same parameters as in the previous examples. The results of the noise reduction are demonstrated in Fig. 3. In Fig. 3(a)–(d), the signal has an SNR of 3 dB, whereas SNR is 0 dB for Fig. 3(e)–(h). According to Fig. 3, the WVD, as expected, is most noisy, whereas among the other three distributions, the presence of white noise is found to be less for the proposed distribution compared with the quadratic CWD.

Moreover, we consider signal energy concentration and bias in terms of instantaneous frequency for a linearly frequency-modulated signal in (42). The energy concentration of the signal is measured by calculating the second-order moment of the TFD with respect to frequency. The resulting standard deviations of the estimated instantaneous frequencies σ_{in} show the concentration measures and is obtained as

$$\sigma_{\text{in}}^2(n) = \frac{\sum_{k=0}^{K-1} k^2 \rho(n,k)}{\sum_{k=0}^{K-1} \rho(n,k)} - \hat{f}_{\text{in}}^2(n) \tag{43}$$

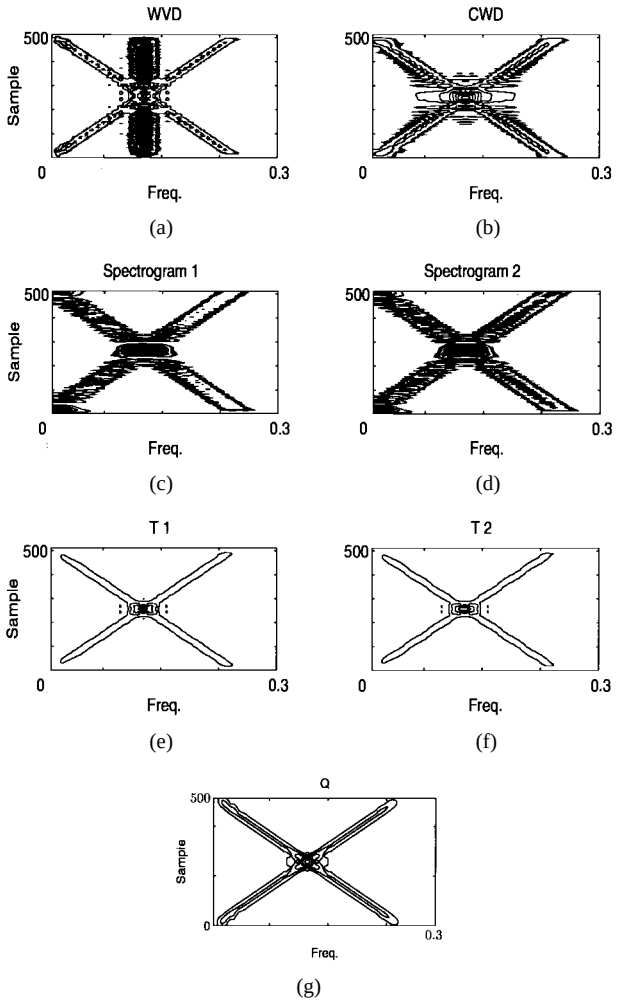

Fig. 2. Cross-term reduction of the WVD by using the CWD, the spectrogram, the proposed time–frequency representation, and a smoothed pseudo-Wigner–Ville distribution. (a)–(g) Contour plots ($L = 32$).

where $\rho(n, k)$ is the TFD, and $\hat{f}_{\text{in}}(n)$ is the estimated instantaneous frequency defined as the periodic first moment of $\rho(n, k)$ with respect to frequency [1]. In (43) the subscript "in" stands for instantaneous frequency. The bias, as a function of time, is defined as the absolute difference between true and estimated instantaneous frequencies. One of the linearly frequency-modulated signal in (42) is analyzed, and the parameters used are $L = 32$ and $K = 128$. For the proposed TFD, the concentration and bias as a function of time are found high (since $\sigma_{\text{in}}^2(n)$ is low) and low, respectively, compared with the results obtained by using only filter banks, and are quite close to the results of the WVD. The filter bank with $|H(f)|^2$ in (40) provides a slightly higher standard deviation and lower bias than using $|H(f)|^2$ in (41).

Example 2—Effects for Artifacts: To illustrate the effects of artifacts, we consider a nonlinearly frequency-modulated signal

$$z(n) = e^{j(w_0 n + 2\pi\rho\cos(w_m n))}$$

where

$$w_0 = \pi/4, \quad \rho = 2, \quad w_m = 0.01\pi \qquad -(N-1)/2 \le n \le (N-1)/2. \tag{44}$$

The impulse response corresponding to (40) is used as the window function for the spectrogram. The parameter σ for the CWD is 0.5, the order q of the GWVD is 2, and the number of filters L is 16. The corresponding results for different distributions are presented in

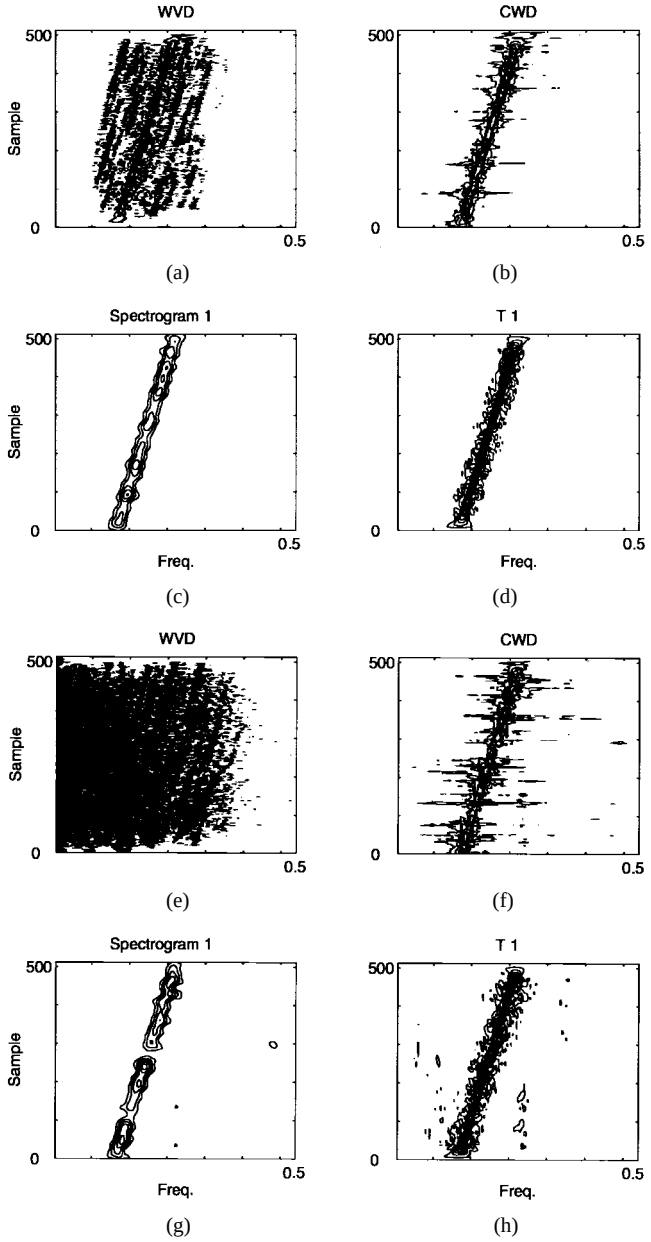

Fig. 3. Time–frequency representation using the different distributions for a noisy linear chirp with (a)–(d) SNR = 3 dB and (e)–(h) SNR = 0 dB ($L = 32$).

Fig. 4. In Fig. 4(a)–(d), the WVD, spectrogram, GWVD, and CWD are shown, whereas the proposed TFD with WVD's and GWVD's are shown in Fig. 4(e)–(f), respectively. As we can see, the energy concentration for the proposed distribution is higher, and the presence of artifacts is lower than in the other distributions. Furthermore, the proposed TFD with GWVD's provides a higher concentration than with the use of WVD's [cf. Fig. 4(e)–(f)].

Example 3—Signal Reconstruction: We illustrate an example of signal reconstruction by using a linearly frequency-modulated signal that has normalized frequency (with respect to the sampling frequency) increasing linearly with time from 0.1 to 0.2. The number of filters used is $L = 16$, and the parameters used for the pulse $p(t)$ are $\alpha = 0.5$ and $\beta = 1.1$. The corresponding value of β gives small variations of $p(t)$ with respect to the frequency. In Fig. 5(a)–(c), the true signal and the reconstructed signals are presented. Comparing Fig. 5(b) and (c) with Fig. 5(a), an improvement in reconstruction has

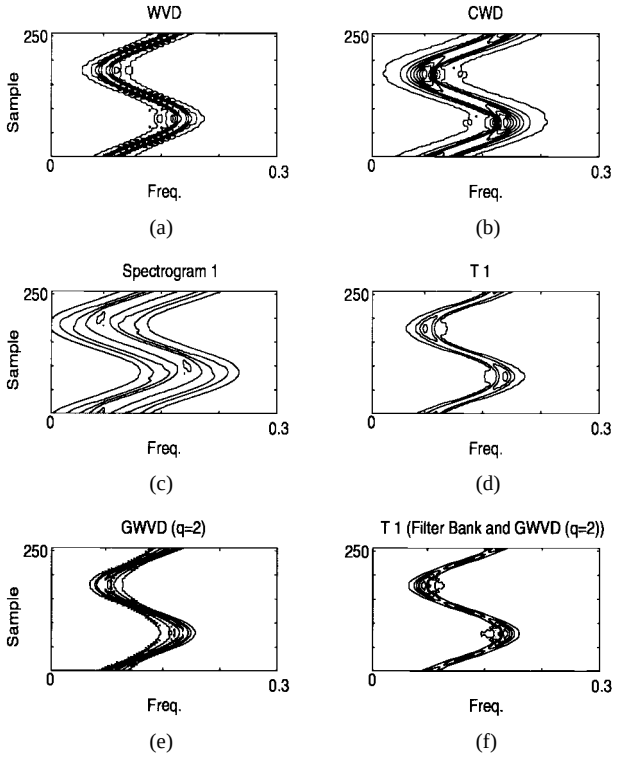

Fig. 4. Time–frequency representation of a nonlinearly frequency modualted signal using different distributions ($L = 16$).

been attained according to Fig. 5(c). The filtering effect of $G(t, f)$ is removed by the inverse filter $b(t, f)$, providing the result that is quite close to the result from the WVD. This can be shown by calculating the mean-squared error (MSE) between the true signal $s(n)$ and reconstructed signal $\hat{s}(n)$ of length M as MSE $= 1/M(\Sigma_{n=1}^{M}(s(n) - \hat{s}(n))^2)$, which are MSE $= 0.405$ and MSE $= 0.579$, as obtained for Fig. 5(a) and (c), respectively, which are small and close compared with the MSE ($= 6.05$) for Fig. 5(b). Note that the signal enhancement can be performed in the case of a noisy signal. In order to separate noise, the time–frequency plane can be masked by a time-varying window, e.g., a Gaussian window, and the following reconstruction will give an enhanced signal.

IV. Conclusion

We have proposed a method for TFA of nonstationary signals using the combination of filter bank and WVD's. The method is efficient for cross-term reduction and noise suppression and provides high energy concentration of the signal since both linear and nonlinear operations are involved. Moreover, the bias and the variance in terms of instantaneous frequency are low. The method behaves like the spectrogram when the subfilters are narrowbanded and like the WVD when the filters are widebanded. It provides some of the desirable properties of the TFD and can be used to design a kernel. Moreover, an approximate method based on the inverse of the kernel has been suggested for signal reconstruction. Several numerical examples for different nonstationary signals and white Gaussian noise are given, demonstrating the performace of the TFD. The results are also compared with the Choi–Williams distribution, the spectrogram, and a smoothed pseudo-WVD. For nonlinearly frequency-modulated signals or non-Gaussian noise, the higher order GWVD can be used. The method has an advantage over other methods for TFR in that it can provide masking in the time–frequency plane by the choice of filters. Tiling of the time–frequency plane may be possible by

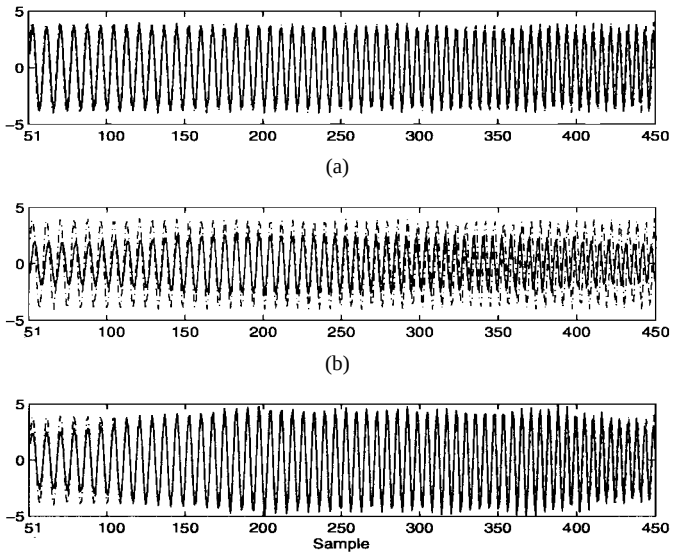

Fig. 5. Signal reconstruction from the time–frequency plane. (a)–(c) True signal (dashed-dot line) and the corresponding reconstructed signals (solid line) from (a) WVD, (b) $T(t,f)$, and (c) $T(t,f) * b(t,f)$, respectively.

considering various transforms. Various applications, for example, the estimation of instantaneous frequencies, signal enhancement, and signal separation, can be made for nonstationary signals.

Appendix A

Reality

The kernel $G(t, f-\overline{f})$ is real because the complex conjugate of $G(t, f-\overline{f})$ is

$$\begin{aligned} G^*(t, f-\overline{f}) &= \int h(t+\eta/2)h(t-\eta/2) \\ &\quad \cdot \frac{\sin \pi M\eta/L}{\sin \pi\eta/L} e^{j2\pi(f-\overline{f})\eta}\, d\eta \\ &= \int_{-\infty}^{\infty} h(t+\eta/2)h(t-\eta/2) \\ &\quad \cdot \frac{\sin \pi M\eta/L}{\sin \pi\eta/L} e^{-j2\pi(f-\overline{f})\eta}\, d\eta \\ &\quad \cdot \begin{pmatrix}\text{substituting -}\eta\text{ for }\eta \\ \text{and changing the integral limit}\end{pmatrix} \\ &= G(t, f-\overline{f}). \end{aligned} \tag{A.1}$$

Similarly, the TFD $T(t,f)$ in (14) is real since $W_s(t,f)$, which is the WVD of the signal $s(t)$, is also real [2].

Marginals

Frequency Marginal: In the following, the frequency marginal of the TFD, which is given in (18), is derived. Using (13) and then replacing (10), (18) can be written as

$$\begin{aligned} \int T(t,f)\, dt &= \sum_{i=1}^{M} \int W_i(t,f)\, dt \\ &= \sum_{i=1}^{M} \iint s(u+\xi/2)s^*(u-\xi/2) \\ &\quad \cdot \left[\int G_i(t-u, f-f_i)\, dt\right] \\ &\quad \cdot e^{-j2\pi f\xi}\, du\, d\xi. \end{aligned} \tag{A.2}$$

From (11), we get

$$\begin{aligned} &\int G_i(t-u, f-f_i)\, dt \\ &\quad = \iint h(t-u+\eta/2)h(t-u-\eta/2)e^{-j2\pi(f-f_i)\eta}\, d\eta dt \\ &\quad = \int \left[\int h(\tau+\eta)h(\tau)\, d\tau\right] e^{-j2\pi(f-f_i)\eta}\, d\eta \\ &\qquad (\text{considering } t-u-\eta/2=\tau) \\ &\quad = \int r_h(\eta)e^{-j2\pi(f-f_i)\eta}\, d\eta = |H(f-f_i)|^2. \end{aligned} \tag{A.3}$$

By variable substitution, we also get

$$\int s(u+\xi/2)s(u-\xi/2)\, du = r_s(\xi). \tag{A.4}$$

Finally, inserting (A.3) and (A.4) into (A.2), we can obtain (A.2) as

$$\begin{aligned} \int T(t,f)\, dt &= \sum_{i=1}^{M} |H(f-f_i)|^2 \int r_s(\xi)e^{-j2\pi f\xi}\, d\xi \\ &= \sum_{i=1}^{M} |H(f-f_i)|^2 |S_s(f)|^2 \\ &= |S_s(f)|^2 \sum_{i=1}^{M} |H(f-f_i)|^2, \qquad f>0. \end{aligned} \tag{A.5}$$

Thus, according to (A.5), the frequency marginal (18) is fulfilled only if

$$\sum_{i=1}^{M} |H(f-f_i)|^2 = 1, \qquad 0<f<M/L. \tag{A.6}$$

Time Marginal: In order to obtain the time marginal, we integrate the TFD over frequency and find

$$\begin{aligned} P(t) = \int T(t,f)\, df &= \sum_{i=0}^{2M} \int W_i(t,f)\, df \\ &= \sum_{i=0}^{2M} |z_i(t)|^2. \end{aligned} \tag{A.7}$$

The last quantity is valid since each TFD $W_i(t,f)$ is a WVD, and the number of subfilters for convenience is chosen to be $2M+1$. Using (3), (A.7) can be obtained as

$$\begin{aligned} P(t) = \sum_{i=0}^{2M} |z_i(t)|^2 &= \iint s(t-\xi_1)s(t-\xi_2)h(\xi_1)h(\xi_2) \\ &\quad \cdot \sum_{i=0}^{2M} e^{-j2\pi i(\xi_2-\xi_1)/L}\, d\xi_1, d\xi_2 \end{aligned} \tag{A.8}$$

where $f_i = i/L$, $i=0,1,\cdots,2M$. By rewriting the sum as

$$\begin{aligned} &\sum_{i=0}^{2M} e^{-j2\pi i(\xi_2-\xi_1)/L} \\ &\qquad = e^{-j2\pi(\xi_2-\xi_1)M/L} \sum_{i=-M}^{M} e^{-j2\pi i(\xi_2-\xi_1)/L} \end{aligned} \tag{A.9}$$

the Poisson's sum formula can be used. For large M, (A.9) can be approximately expressed as

$$\begin{aligned} &e^{-j2\pi(\xi_2-\xi_1)M/L} \sum_{i=-M}^{M} e^{-j2\pi i(\xi_2-\xi_1)/L} \\ &\qquad \to M \to \infty L \sum_{l=-\infty}^{\infty} \delta(\xi_2-\xi_1+lL) \end{aligned} \tag{A.10}$$

where the phase factor $e^{-j2\pi(\xi_2-\xi_1)M/L}$ will be equal to one whenever $(\xi_2-\xi_1)=lL$. Inserting (A.10) into (A.8) gives

$$\begin{aligned} P(t) &= L\sum_l \int s(t-\xi_1+lL)s(t-\xi_1)h(\xi_1) \\ &\quad \cdot h(\xi_1-lL)\,d\xi_1 \\ &\approx L\int s^2(t-\xi)h^2(\xi)\,d\xi \end{aligned} \tag{A.11}$$

since the lth terms decrease rapidly, and a significant contribution will be obtained only for $l=0$. If $|h(\xi)|\approx 0$, $|\xi|>L$, and $s(t)$ is sufficiently smooth for $|t|<L$, then

$$\begin{aligned} P(t) &\approx s^2(t)L\int h^2(\xi)\,d\xi \\ &= s^2(t)L\int_{-1/L}^{1/L}|H(f)|^2\,df \\ &= s^2(t)\int_{-1/2}^{1/2}\sum_{i=-L/2}^{L/2}|H(f-f_i)|^2\,df \end{aligned} \tag{A.12}$$

is valid. Thus, the time marginal is approximately valid as

$$P(t)\approx s^2(t) \tag{A.13}$$

if $s(t)$ is sufficiently smooth within $|t|<L$ and $\Sigma_{i=-L/2}^{L/2}|H(f-f_i)|^2=1, |f|<1/2$, provided the time width of the impulse response $h(t)$ is small, i.e., the bandwidth of the prototype filter is reasonably large.

ACKNOWLEDGMENT

The authors are greatly acknowledged for the valuable comments and suggestions of the anonymous reviewers and the Associate Editor Dr. N. Erdol.

REFERENCES

[1] B. Boashash, "Time-frequency signal analysis," *Advances in Spectral Estimation and Array Proc.*, vol. 1, S. Haykin, Ed. Englewood Cliffs, NJ: Prentice-Hall, 1991, ch. 9, pp. 418–517.

[2] L. Cohen, *Time-Frequency Analysis*. Englewood Cliffs, NJ: Prentice-Hall, 1995.

[3] I. Choi and W. Williams, "Improved time-frequency representation of multicomponent signals using exponential kernels," *IEEE Trans. Acoust., Speech, Signal Processing*, vol. 37, pp. 862–871, June 1989.

[4] L. Stanković and S. Stanković,"An analysis of instantaneous frequency representations using time-frequency distributions-generalized Wigner distribution," *IEEE Trans. Signal Processing*, vol. 43, pp. 549–552, Feb. 1995.

[5] B. Boashash, Ed., *Time-Frequency Signal Analysis—Methods and Applications*. Melbourne, Australia: Longman-Cheshire, Wiley, 1992.

[6] F. Hlawatsch and G. F. Boudreaux-Bartels,"Linear and quadratic time-frequency signal representations," *IEEE Signal Processing Mag.*, pp. 21–66, Apr. 1992.

[7] L. R. Rabiner and R. W. Schafer, *Digital Signal Processing of Speech Signals*. Englewood Cliffs, NJ: Prentice-Hall, 1978.

[8] J. Jeong and W. J. Williams, "Kernel design for reduced interference distributions," *IEEE Trans. Signal Processing*, vol. 40, pp. 402–412, Feb. 1992.

[9] L. L. Scharf, *Statistical Signal Processing: Detection, Estimation, and Time-Series Analysis*. Reading. MA: Addison-Wesley, 1991.

[10] G. F. Boudreaux-Bartels and T. W. Parks, "Time-varying filtering and signal estimation using Wigner distribution synthesis techniques," *IEEE Trans. Acoust., Speech, Signal Processing*, vol. 34, pp. 442–451, June 1986.

[11] P. P. Vaidyanathan, *Multirate Systems and Filter Banks*. Englewood Cliffs, NJ: Prentice-Hall, 1993.

[12] ——, "Theory and design of M-channel maximally decimated quadrature mirror filters with arbitrary M, having the perfect reconstruction property," *IEEE Trans. Acoust., Speech, Signal Processing*, vol. ASSP-35, pp. 476–492, Apr. 1987.

[13] M. Vetterli and D. Le Gall, "Perfect reconstruction FIR filter banks: Some properties and factorizations," *IEEE Trans. Acoust., Speech, Signal Processing*, vol. 37, pp. 1057–1071, July 1989.

[14] R. G. Baraniuk and D. L. Jones, "New signal-space orthogonal bases via the metaplectic transform," in *Proc. IEEE-SP Symp. Time–Freq. Time–Scale Anal.*, Victoria, B.C., Canada, Oct. 1992, pp. 339–342.

Channel Equalization for Coded Signals in Hostile Environments

Kristina Georgoulakis and Sergios Theodoridis

***Abstract*— In this correspondence, the detection of trellis-coded modulated signals corrupted by intersymbol interference, co-channel interference, and nonlinear impairments is treated as a classification task by means of a clustering based sequence equalizer decoder. The receiver performs jointly decoding and equalization of trellis-encoded signals. No specific model is required for the channel or for the interference and the noise, and no code knowledge is needed at the receiver. Complexity reduction of the equalizer is obtained through two suboptimal techniques: a) clusters' grouping and b) the *M* algorithm. The robust performance of the proposed scheme is illustrated by simulations.**

***Index Terms*— Cochannel interference, equalizers, nonlinearities, Trellis-coded modulation.**

I. INTRODUCTION

Trellis-coded modulation (TCM) is a combined coding and modulation scheme, which improves the noise immunity of a digital transmission system without increasing the transmitted power or the required bandwidth [1]. Thus, TCM is a very attractive transmission scheme for modern communication systems, where power and bandwidth efficiency is required.

However, these systems suffer from the presence of different impairments, such as intersymbol interference (ISI), co-channel interference (CCI), and channel nonlinearities [2], [3]. For example, in satellite communications, where TCM is widely used, system performance is reduced due to CCI coming from adjacent beams and adjacent satellites. Furthermore, because of the limited availability of bandwidth, the transmitted signals must be severely bandlimited, and this is a source of ISI [3], [4]. In radio mobile communications, the same impairments appear due to frequency reuse (CCI) and multipath propagation (ISI). In addition, nonlinear signal impairments arise from signal companding in telephone transmission or in amplification processes whenever amplifiers are operated near the saturation point (for example, in satellite communications) [4].

For the suppression of ISI in TCM systems, many different approaches have been investigated. Equalization and decoding procedures are performed either separately [5] or jointly [6]. The

Manuscript received October 22, 1997; revised October 12, 1998. The associate editor coordinating the review of this paper and approving it for publication was Dr. Jose C. Principe.

The authors are with the Department of Informatics, University of Athens, Athens, Greece (e-mail: stheodor@di.uoa.gr).

Publisher Item Identifier S 1053-587X(99)03638-7.